J Fusion Energ (2015) 34:379–385
DOI 10.1007/s10894-014-9809-z

ORIGINAL RESEARCH

Reaction Cross-Section, Stopping Power and Penetrating Distance Calculations for the Structural Fusion Material ^{54}Fe in Different Reactions

H. Özdoğan · V. Çapalı · A. Kaplan

Published online: 23 November 2014

Abstract Nuclear reaction codes give us simplicity to investigate phenomena of nuclear physics. There have many computer programs such as TALYS, EMPIRE, ALICE/ASH, PCROSS, FLUKA and GEANT4. The stopping power of alpha, deuteron, proton and triton in ^{54}Fe materials is acquired as it has helpful applications of shielding and choosing the proper thickness of the target. Level density is very important to understanding nuclear reaction mechanism. The knowledge of level density for reaction cross-section calculations are required for various application such as astrophysics, accelerator driven sub-critical systems, nuclear medicine, fission and fusion reactor design and neutron capture. In this study, we calculated the cross-sections of ^{54}Fe using TALYS 1.6 and EMPIRE 3.1 codes for different reactions through the four level density models. Stopping powers and penetrating distances were calculated for the alpha, deuteron, proton and triton particles, taking into consideration all possible reactions in ^{54}Fe for incident energies of 1–45 MeV using GEANT4 calculation code. The obtained reaction cross-section results have been compared with the each other and against the experimental nuclear reaction data existing in EXFOR database.

Keywords Reaction cross-section · Level density · GEANT4 · Stopping power · Iron · EXFOR file

H. Özdoğan · V. Çapalı · A. Kaplan
Department of Physics, Faculty of Arts and Sciences, Süleyman Demirel University, Isparta, Turkey

H. Özdoğan (✉)
Department of Biophysics, Faculty of Medicine, Akdeniz University, Antalya, Turkey
e-mail: hasanozdogan@akdeniz.edu.tr

Introduction

The most important problem of today's world is to obtain clean and safe energy. Scientists have sought on this problem since middle of twentieth century. The fusion materials development for the safety of fusion reactors is very important. A good realizing on the mechanical properties and microstructure change of materials under effect of radiation is of great important for performing a safe design and operation of new nuclear systems and for developing structural materials in fusion power plants [1]. An extraordinary importance is being given for the structural materials development because the achievement of the fusion reactors is mainly dependent on the development of these materials. The development of suitable structural materials is an important stage towards fusion reactors becoming an effective energy source, especially if the promise of an environmentally free of risk machine is to be understood. The selection of structural materials for combined first-wall-breeding blanket parts depends not only on mechanical properties, suitability with other materials, nuclear properties and irradiation performance, but also on their radiological properties [2–5].

The process of simulation programs and nuclear reaction codes gave us the chance to design virtual experimental conditions to simulate phenomena of nuclear physics. The cross-section calculations, spectrum analyzes of outgoing particles and dosimeter calculations can be given example this situation. Estimating of reaction cross-section remains a major problem in applications such as data evaluations. There has been much progress in the development of nuclear reaction codes, which now include different reaction mechanisms to take care of [6].

The reaction cross-section data have a critical importance on fusion reactors and development of fusion reactor technology. In a fusion reactor design, neutron reaction cross-section data are needed and the evaluated values in nuclear data files are generally used for neutronic calculations [7–9]. The theoretical nuclear reaction models are usually required to get the prediction of the reaction cross-sections, specifically if the experimental data are unavailable or are improbably to be produced because of the experimental troubles [10–16].

Level density is a characteristic property of every nucleus and it is defined as the number of levels per unit energy at certain excitation energy. In other words it is the number of different ways in which individual nucleons can be placed in the various single particle orbitals such that the excitation energy lies in the range E to $E + dE$. It increases rapidly with excitation energy. Level density is crucial to understanding nuclear reaction mechanism. The knowledge of level density for reaction cross-section calculations are required for various application such as astrophysics, accelerator driven sub-critical systems, nuclear medicine, fission and fusion reactor design and neutron capture [17].

The stopping power of matter for charged particles such as proton, alpha, deuteron is very crucial in reactor applications and dosimeter calculations. It is also useful in understanding the interaction of particles with matter. The heavy charged particles like proton interact with matter primarily through coulomb forces between positive and negative charge of the orbital electrons within the absorber atoms [18].

In this paper, we calculated the cross-sections of ^{54}Fe using TALYS 1.6 [19] and EMPIRE 3.1 [20, 21] codes for different reactions through the four level density models. Also, stopping power and penetrating distances of ^{54}Fe for some charged particles have been calculated using GEANT4 [22] code. The obtained reaction cross-section results have been compared with the each other and against the National Nuclear Data Center (EXFOR) [23] database.

Calculation Methods

The reaction cross-sections of ^{54}Fe target nucleus have been calculated using Constant Temperature Fermi Gas Model (CTM), Back Shifted Fermi Gas Model (BSFM) and Generalized Superfluid Model (GSM) for the TALYS 1.6 and Default Model for the EMPIRE 3.1 computer codes.

The TALYS is a nuclear reaction simulation code for the analysis and estimation of nuclear reactions that include neutrons, protons, photons, tritons, deuterons, ^{3}He and alpha particles in the energy range of 1 keV–1 GeV. For this, TALYS integrates the optical model, pre-equilibrium, direct, fission and statistical nuclear reaction models in one calculation plan and in that connection gives a prediction for all the possible reaction. In TALYS, various options are contained for the select of various parameters such as level density, gamma strength function and compound nuclear model parameters [24]. The default cross-section calculations were considered by the two-component exciton model [25]. This model is based on the Kalbach's theory [26]. The proton and neutron type of the produced particles and holes is clearly followed during the reaction in the two-component exciton model.

The EMPIRE 3.1 contains the mechanism of pre-equilibrium as explained in the exciton model [27], as dependent upon the master equation solution [28] in the form recommended by Cline [29] and Ribansky [30]

$$-q_{t=0}(n) = \lambda_+(E, n+2)\tau(n+2) + \lambda_-(E, n-2)\tau(n-2) - [\lambda_+(E, n) + \lambda_+(E, n) + L(E, n)]\tau(n) \quad (1)$$

where $q_t(n)$ is the initial occupation probability of the composite nucleus in the state with the exciton number n, $\lambda_+(E, n)$ and $\lambda_-(E, n)$ are the transition rates for decay to neighboring states, and $L(E,n)$ is the total emission rate integrated over emission energy for particles (neutrons υ, protons π and clusters) and γ-rays. The pre-equilibrium spectra can be calculated as.

$$\frac{d\sigma_{a,b}}{d\varepsilon_b}(\varepsilon_b) = \sigma^r_{a,b}(E_{inc})D_{a,b}(E_{inc}) \times \sum_n W_b(E, n, \varepsilon_b)\tau(n) \quad (2)$$

where $\sigma^r_{a,b}(E_{inc})$ is the cross-section of the reaction (*a*, *b*), $W_b(E, n, \varepsilon_b)$ is the probability of emission of a particle of type *b* (or γ-ray) with energy ε_b from a state with *n* excitons and excitation energy *E* of the compound nucleus, and $D_{a,b}(E_{inc})$ is the depletion factor, which takes into account the flux loss as a result of the direct reaction processes.

In the BSFM [31], the pairing energy is treated as an adjustable parameter and the Fermi gas expression is used all the way down to 0 MeV. However, it should be noted that standard version of the Fermi gas expression at low excitation energies leads to numerical divergence.

The CTM [32] requires solving the problem of matching the constant temperature part at low energies and the Fermi gas expression at high energies. Since this matching depends on experimental information (discrete levels, mean resonance spacings, shell corrections, separation energies, etc.) it may occur that the solution of the matching problem yields hard to believe, and sometimes unphysical, values for the matching parameters.

The GSM takes superconductive pairing correlations into account according to the Bardeen–Cooper–Schrieffer theory. The phenomenological version of the model [33, 34] is characterized by a phase transition from a superfluid behavior at low energy, where pairing correlations strongly influence the level density, to a high-energy region that is described by the FGM. The GSM thus resembles the CTM to the extent that it distinguishes between a low energy and a high-energy region, although for the GSM this distinction follows naturally from the theory and does not depend on specific discrete levels that determine a matching energy. Instead, the model automatically provides a constant temperature-like behavior at low energies.

GEANT4 is a free simulation and calculation code that can be used to investigation of high-energy physics, medical physics, space and radiation physics. At the heart of GEANT4 is an abundant set of physics models to handle the interactions of particles with matter across a very wide energy range. Data and expertise have been drawn from many sources around the world and in this respect, GEANT4 acts as a repository that incorporates a large part of all that is known about particle interactions [22].

The GEANT4 processes are dedicated to stopping power into ^{54}Fe. Stopping powers and penetrating distances in material for different reactions were calculated for the incident alpha, deuteron, proton and triton particles, taking into consideration all possible reactions such as ionization, scattering, absorption, transmission and charge transfer in ^{54}Fe for incident energies of 1–45 MeV using by Bethe Bloch's and Niels Bohr's approximation [35, 36].

Results and Discussion

In the present study, the reaction cross-sections of $^{54}Fe(\alpha,n)^{57}Ni$, $^{54}Fe(\alpha,2n)^{56}Ni$, $^{54}Fe(d,n)^{55}Co$, $^{54}Fe(d,\alpha)^{52}Mn$, $^{54}Fe(n,2n)^{53}Fe$, $^{54}Fe(n,\alpha)^{51}Cr$, $^{54}Fe(n,p)^{54}Mn$ and $^{54}Fe(p,\alpha)^{51}Mn$ reactions have been calculated for different level density models using TALYS 1.6 and EMPIRE 3.1 computer codes. The comparison of the calculated and experimental reaction cross-sections have been shown in Figs. 1, 2, 3, 4, 5, 6, 7 and 8. All experimental data used in this study have been taken from the Ref. [23].

The calculated cross-sections of $^{54}Fe(\alpha,n)^{57}Ni$ reaction have been compared with the experimental data in Fig. 1. The TALYS 1.6 CTM and BSFM model calculations are in good agreement the experimental results up to 17 MeV. The TALYS 1.6 GSM model calculations are in good harmony with the experimental data except in the 17–27 MeV alpha energy region. EMPIRE 3.1 Default Model calculations exhibit a little discrepancy with the experimental data up to 27 MeV. The comparison of calculated cross-sections of $^{54}Fe(\alpha,2n)^{56}Ni$ reaction with the experimental values shown in Fig. 2. The TALYS 1.6 CTM and BSFM model results are in good harmony with the experimental results but they follow experimental data from above in the alpha energy region of 36–41 MeV. EMPIRE 3.1 Default and TALYS 1.6 GSM Model

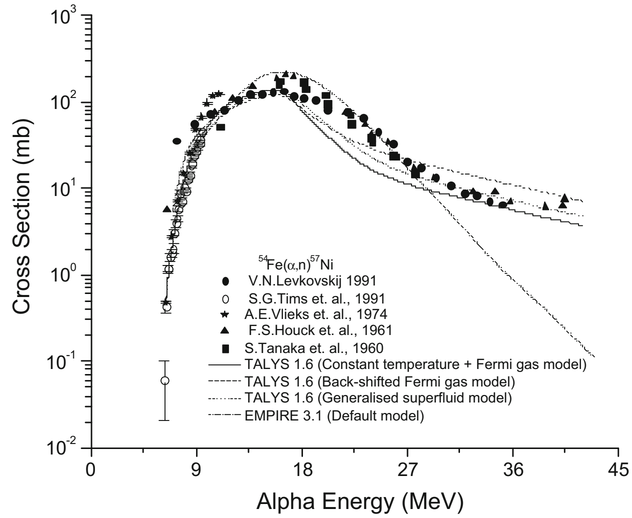

Fig. 1 The comparison of calculated cross-sections of $^{54}Fe(\alpha,n)^{57}Ni$ reaction with the experimental values reported in Ref. [23]

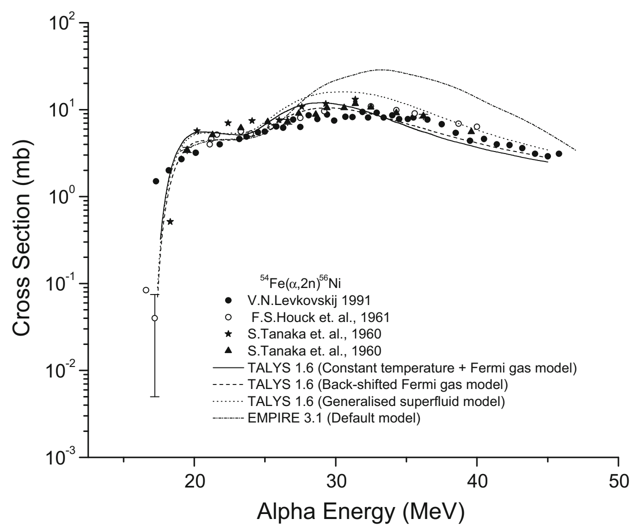

Fig. 2 The comparison of calculated cross-sections of $^{54}Fe(\alpha,2n)^{56}Ni$ reaction with the experimental values reported in Ref. [23]

calculations has similar structure with EXFOR data up to 28 MeV. The $^{54}Fe(d,n)^{55}Co$ reaction cross-section calculations have been compared with the experimental results in Fig. 3. TALYS 1.6 level density models are in good agreement with the experimental values up to 7 MeV deuteron incident energy. After this energy they follow experimental data from below. EMPIRE 3.1 Default Model give similar results with the TALYS 1.6 model calculations up to 7 MeV but this model goes to zero after 8 MeV. The experimental and theoretical results of $^{54}Fe(d,\alpha)^{52}Mn$ reaction have been given in Fig. 4. The cross-section results of the EMPIRE 3.1 Default Model calculations are not in good agreement with the experimental values. They follow the experimental results from above in the

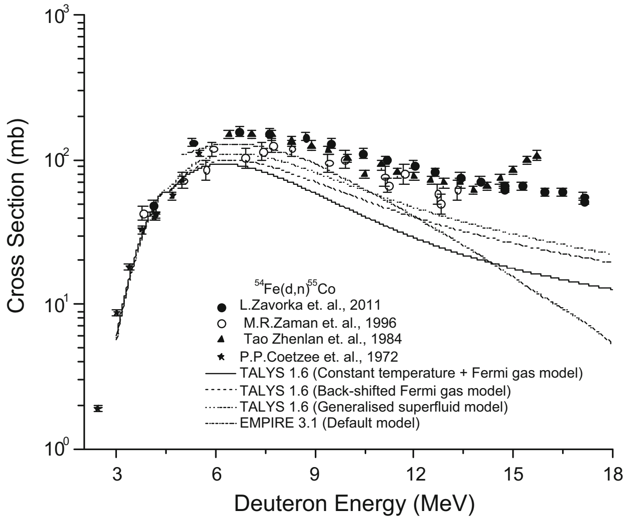

Fig. 3 The comparison of calculated cross-sections of ^{54}Fe(d,n)^{55}Co reaction with the experimental values reported in Ref. [23]

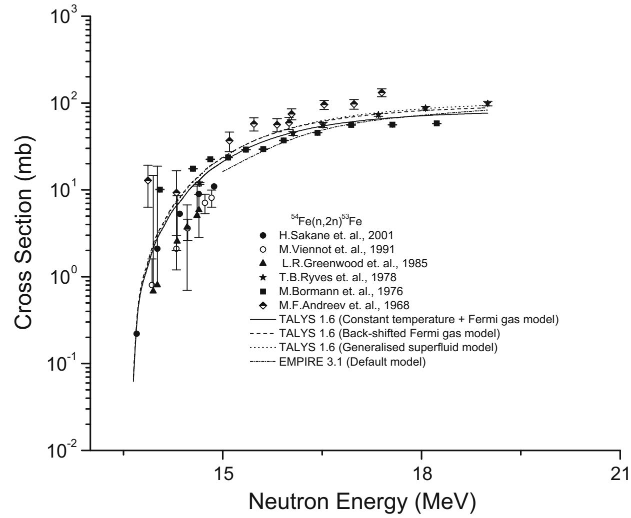

Fig. 5 The comparison of calculated cross-sections of ^{54}Fe(n,2n)^{53}Fe reaction with the experimental values reported in Ref. [23]

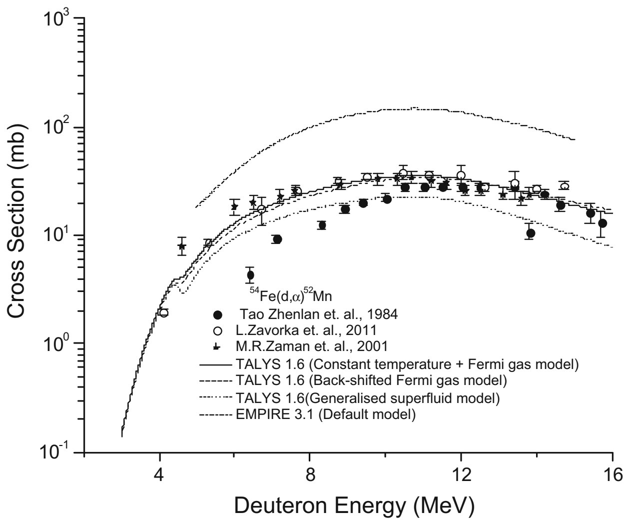

Fig. 4 The comparison of calculated cross-sections of ^{54}Fe(d,α)^{52}Mn reaction with the experimental values reported in Ref. [23]

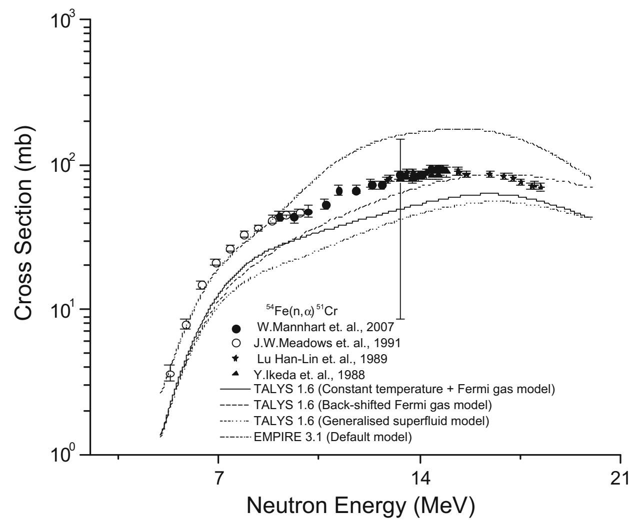

Fig. 6 The comparison of calculated cross-sections of ^{54}Fe(n,α)^{51}Cr reaction with the experimental values reported in Ref. [23]

5–15 MeV incident deuteron energy region. The TALYS 1.6 CTM and BSFM model calculations are in good harmony with the experimental values in the region of all reaction incident energies. The TALYS 1.6 GSM model results give the same geometry with the EXFOR data but they gave different cross-section values in the energy range of 8–14 MeV. The comparison of calculated neutron cross-sections of ^{54}Fe(n,2n)^{53}Fe reaction with the experimental values can be seen in Fig. 5. All level density model calculations are in good harmony with the experimental data. The calculated reaction cross-sections of ^{54}Fe(n,α)^{51}Cr reaction against the EXFOR data have been given in Fig. 6. All the TALYS 1.6 code calculations follow experimental values from below except BSFM model for 15–20 MeV neutron energy region. The EMPIRE 3.1 Default Model calculations are the nearest to the experimental results up to 9 MeV. The comparison of calculated neutron-production cross-sections of ^{54}Fe(n,p)^{54}Mn reaction with the experimental values have been given in Fig. 7. The TALYS 1.6 BSFM and CTM model are in good harmony with the EXFOR values up to 15 MeV but CTM model follow experimental data from below in the neutron energy region of 10–13 MeV. The GSM model of the TALYS 1.6 calculations exhibit a little discrepancy with experimental values up to 7 MeV. The EMPIRE 3.1 Default Model calculations give higher results than the EXFOR data. The reaction cross-section calculations of ^{54}Fe(p,α)^{51}Mn

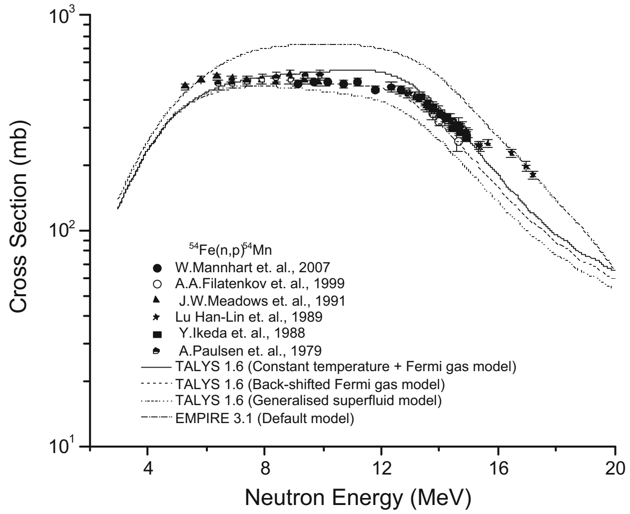

Fig. 7 The comparison of calculated cross-sections of $^{54}Fe(n,p)^{54}Mn$ reaction with the experimental values reported in Ref. [23]

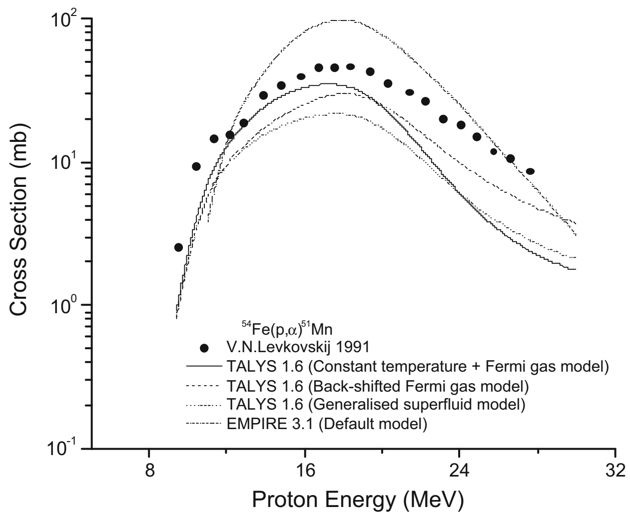

Fig. 8 The comparison of calculated cross-sections of $^{54}Fe(p,\alpha)^{51}Mn$ reaction with the experimental values reported in Ref. [23]

reaction have been shown in Fig. 8. All the TALYS 1.6 level density model calculations follow the experimental results from below while EMPIRE 3.1 Default Model level density calculations follow the experimental data from above after 12 MeV incident proton energy.

Although there are some disagreements between the calculated values and the experimental results, in generally, the TALYS 1.6 CTM and BSFM model cross-section calculations are close to the experimental results except for the Fig. 8. These models can be suggested, if the experimental data are unavailable or are improbably to be produced due to experimental problems.

The penetrating distance calculations of proton, triton, deuteron and alpha particles in the incident energy range of

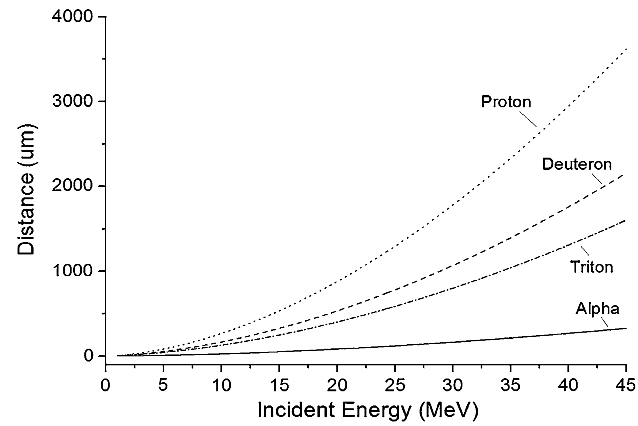

Fig. 9 Alpha, deuteron, proton and triton penetrating distance calculations in ^{54}Fe for incident energies of 1–45 MeV using GEANT4 code

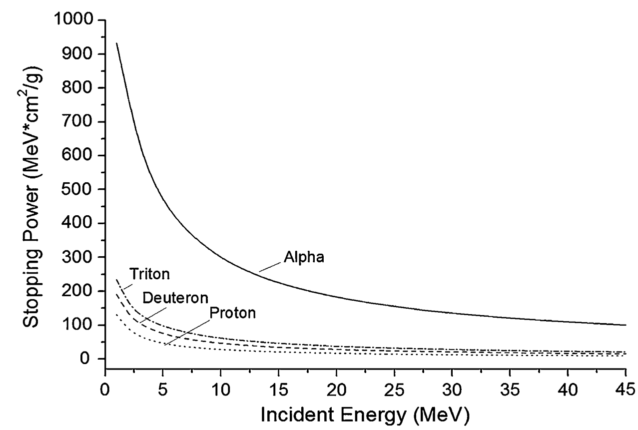

Fig. 10 Alpha, deuteron, proton and triton stopping power calculations in ^{54}Fe for incident energies of 1–45 MeV using GEANT4 code

1–45 MeV for ^{54}Fe structural fusion material shown in Fig. 9. According to calculated results penetrating of alpha particles is the poorest. So this particles cannot be managed to enter into ^{54}Fe. On the contrary alpha particles, proton has the most penetrating in the ^{54}Fe target. As can be seen in Fig. 9, if the mass number of the projectile particles is increased, the penetrating in ^{54}Fe is decreased.

The calculated stopping power values of alpha, deuteron, proton and triton projectile particles in ^{54}Fe target for incident energies of 1–45 MeV have been exhibited in Fig. 10. Bethe Bloch suggested that for high energies above approximately 1 MeV region, the stopping power decreases as the incident particle's energy. All the projectile particles give similar results except for alpha. We note that in the incident energy range of 1–45 MeV proton, deuteron and triton have a far going that exceeds the penetration in ^{54}Fe fusion structural material. All calculated stopping power and penetrating distance results used by GEANT4 have been given in Tables 1 and 2.

Table 1 Alpha, deuteron, proton and triton distances in ^{54}Fe for incident energies of 1–45 MeV

Energy (MeV)	Alpha distances in ^{54}Fe (μm)	Deuteron distances in ^{54}Fe (μm)	Proton distances in ^{54}Fe (μm)	Triton distances in ^{54}Fe (μm)
1	1,211	5,679	6,967	5,500
2	2,602	13,938	19,184	12,137
3	4,422	24,950	36,099	20,920
4	6,634	38,379	57,441	31,526
5	9,205	54,141	82,836	43,781
6	12,108	72,220	112,194	57,617
7	15,328	92,527	145,381	73,007
8	18,855	114,920	182,229	89,950
9	22,683	139,323	222,595	108,434
10	26,808	165,726	266,346	128,405
11	31,227	194,117	313,368	149,798
12	35,936	224,464	363,623	172,553
13	40,924	256,726	417,093	196,650
14	46,185	290,861	473,760	222,083
15	51,709	326,826	533,595	248,850
16	57,490	364,584	596,541	276,943
17	63,527	404,101	662,535	306,353
18	69,818	445,345	731,514	337,059
19	76,362	488,282	803,416	369,044
20	83,159	532,879	878,179	402,288
21	90,206	579,106	955,771	436,772
22	97,503	626,956	1,036,180	472,477
23	105,047	676,423	1,119,380	509,387
24	112,835	727,503	1,205,360	547,485
25	120,864	780,192	1,294,110	586,758
26	129,133	834,483	1,385,600	627,191
27	137,638	890,375	1,479,820	668,768
28	146,376	947,860	1,576,750	711,475
29	155,346	1,006,930	1,676,390	755,297
30	164,545	1,067,580	1,778,700	800,219
31	173,970	1,129,780	1,883,640	846,229
32	183,620	1,193,510	1,991,220	893,323
33	193,492	1,258,780	2,101,400	941,499
34	203,584	1,325,550	2,214,150	990,755
35	213,894	1,393,820	2,329,470	1,041,090
36	224,420	1,463,560	2,447,320	1,092,500
37	235,159	1,534,770	2,567,690	1,144,980
38	246,110	1,607,420	2,690,540	1,198,540
39	257,270	1,681,500	2,815,880	1,253,160
40	268,637	1,757,000	2,943,670	1,308,850
41	280,209	1,833,910	3,073,910	1,365,610
42	291,986	1,912,240	3,206,590	1,423,430
43	303,968	1,991,970	3,341,690	1,482,310
44	316,155	2,073,110	3,479,190	1,542,250
45	328,546	2,155,650	3,619,090	1,603,230

Table 2 Alpha, deuteron, proton and triton stopping power in ^{54}Fe for incident energies of 1–45 MeV

Energy (MeV)	Alpha stopping power in ^{54}Fe (MeV cm^2/g)	Deuteron stopping power in ^{54}Fe (MeV cm^2/g)	Proton stopping power in ^{54}Fe (MeV cm^2/g)	Triton stopping power in ^{54}Fe (MeV cm^2/g)
1	932,200	191,027	130,753	234,545
2	768,043	130,717	87,208	163,285
3	627,857	103,682	66,267	130,600
4	534,935	87,179	54,293	110,945
5	469,695	74,894	46,397	97,306
6	420,899	66,244	40,624	87,087
7	382,658	59,379	36,220	78,537
8	351,565	54,274	32,951	71,641
9	324,139	49,949	30,237	66,171
10	300,343	46,381	28,021	61,338
11	280,867	43,282	26,089	57,598
12	264,270	40,609	24,432	54,214
13	249,487	38,369	23,047	51,244
14	235,993	36,207	21,797	48,618
15	225,328	34,515	20,718	46,327
16	215,122	32,939	19,733	44,211
17	205,881	31,525	18,848	42,299
18	197,479	30,225	18,060	40,561
19	189,977	29,040	17,340	39,067
20	183,018	28,011	16,670	37,490
21	176,531	27,000	16,065	36,165
22	170,531	26,079	15,523	35,040
23	164,964	25,211	15,005	33,930
24	160,166	24,423	14,526	32,900
25	155,331	23,725	14,098	31,929
26	150,811	23,039	13,682	31,041
27	146,155	22,391	13,292	30,190
28	142,199	21,789	12,927	29,389
29	138,858	21,222	12,584	28,634
30	135,448	20,710	12,263	27,977
31	132,211	20,204	11,959	27,291
32	129,165	19,726	11,672	26,653
33	126,243	19,272	11,400	26,048
34	123,549	18,841	11,143	25,455
35	120,912	18,443	10,904	24,915
36	118,399	18,053	10,672	24,394
37	116,001	17,692	10,451	23,936
38	113,712	17,337	10,251	23,463
39	111,749	16,998	10,050	23,011
40	109,600	16,673	9,857	22,578
41	107,593	16,363	9,673	22,160
42	105,668	16,078	9,496	21,763
43	103,819	15,792	9,372	21,382

Table 2 continued

Energy (MeV)	Alpha stopping power in ^{54}Fe (MeV cm^2/g)	Deuteron stopping power in ^{54}Fe (MeV cm^2/g)	Proton stopping power in ^{54}Fe (MeV cm^2/g)	Triton stopping power in ^{54}Fe (MeV cm^2/g)
44	102,043	15,517	9,165	21,038
45	100,259	15,253	9,010	20,685

Summary and Conclusions

In this study, the reaction cross-section of ^{54}Fe reactions have been calculated for the different level density models using the TALYS 1.6 and EMPIRE 3.1 codes. The theoretical calculation results have been also compared with the obtainable experimental data in the EXFOR database. Also, stopping power and distance of penetrating in ^{54}Fe target using by GEANT4 have been simulated. The results can be summarized and concluded as follows:

1. Generally the calculated reaction cross-sections of ^{54}Fe reactions are in agreement with the experimental data for the TALYS 1.6 CTM and BSFM model results.
2. The TALYS 1.6 GSM and EMPIRE 3.1 Default model calculations show some disparateness with the EXFOR values for all reactions investigated in this study.
3. The TALYS 1.6 CTM and BSFM option for ^{54}Fe reaction cross-section calculations can be chosen, if the experimental data are unavailable or are improbably to be produced because of the experimental troubles.
4. In the incident energy range of 1–45 MeV, required target thickness of ^{54}Fe could be stopped alpha, triton, deuteron and proton, approximately 328, 1,603, 2,155, 3,619 μm respectively.
5. The obtained ^{54}Fe stopping power results for the projectile charged particles can be used in several applications such as fusion reactor design and shielding.

References

1. P.P. Liu et al., J. Alloys Compd. **579**, 599 (2013)
2. P.M. Raole et al., Trans. IIM **62**, 2 (2009)
3. M. Victoria et al., Nucl. Fusion **41**, 1047 (2001)
4. K. Ehrlich, Philos. Trans. R. Soc. Lond. A **357**, 595 (1999)
5. A. Kaplan et al., J. Fusion Energ. **29**, 353 (2010)
6. A. Kaplan et al., J. Fusion Energ. **33**, 510 (2014)
7. H. Aytekin et al., J. Fusion Energ. **30**, 21 (2011)
8. T. Nishio et al., J. Nucl. Sci. Technol. **2**, 955 (2002)
9. A. Kaplan et al., J. Fusion Energ. **32**, 344 (2013)
10. E. Tel et al., J. Fusion Energ. **32**, 304 (2013)
11. A. Kaplan, J. Fusion Energ. **32**, 382 (2013)
12. A. Kaplan et al., J. Fusion Energ. **32**, 431 (2013)
13. H. Aytekin et al., J. Radioanal. Nucl. Chem. **298**, 95 (2013)
14. A. Aydın et al., J. Fusion Energ. **27**, 308 (2008)
15. E. Tel et al., J. Fusion Energ. **31**, 184 (2012)
16. A. Kaplan, V. Çapalı, J. Fusion Energ. **33**, 299 (2014)
17. A.J. Koning et al., Nucl. Phys. A. **810**, 13 (2008)
18. V. Yadav et al., Proc. DAE Symp. Nucl. Phys. **57**, 734 (2012)
19. A. Koning, S. Hilaire, S. Goriely, TALYS–1.6 A Nuclear Reaction Program, User Manual (NRG, The Netherlands), First Edition, December 23 (2013)
20. M. Herman et al., Nucl. Data Sheets **108**, 2655 (2007)
21. M. Herman et al., EMPIRE–3.1 Rivoli Modular System for Nuclear Reaction Calculations and Nuclear Data Evaluation, User's Manual (2012)
22. S. Agostinelli et al., Nucl. Instrum. Methods Phys. Res. A. **506**, 250 (2003)
23. Brookhaven National Laboratory, National Nuclear Data Center, EXFOR/CSISRS (Experimental Nuclear Reaction Data File). Database Version of November 20, 2013 (2013), http://www.nndc.bnl.gov/exfor/
24. R. Crasta et al., J. Radioanal. Nucl. Chem. **290**, 367 (2011)
25. A.J. Koning, M.C. Duijvestijn, Nucl. Phys. A **744**, 15 (2004)
26. C. Kalbach, Phys. Rev. C **33**, 818 (1986)
27. J.J. Griffin, Phys. Rev. Lett. **17**, 478 (1966)
28. C. Cline, M. Blann, Nucl. Phys. A **172**, 225 (1971)
29. C.K. Cline, Nucl. Phys. A **193**, 417 (1972)
30. I. Ribansky et al., Nucl. Phys. A **205**, 545 (1973)
31. W. Dilg et al., Nucl. Phys. A **217**, 269 (1973)
32. A. Gilbert, A.G.W. Cameron, Can. J. Phys. **43**, 1446 (1965)
33. A.V. Ignatyuk et al., Sov. J. Nucl. Phys. **29**, 450 (1979)
34. A.V. Ignatyuk et al., Phys. Rev. **C47**, 1504 (1993)
35. H. Bethe, Ann. Phys. **5**, 325 (1930)
36. M. Inokuti, Rev. Mod. Phys. **43**, 297 (1971)